Implicit Normal Mode Initialization for an Operational Regional Model

CLIVE TEMPERTON AND MICHEL ROCH

Recherche en Prévision Numérique, Atmospheric Environment Service, Dorval, Québec, Canada

(Manuscript received 4 May 1990, in final form 6 September 1990)

ABSTRACT

In a previous study based on the shallow-water equations, it was shown that nonlinear normal mode initialization (NMI) can be implemented without knowing the normal modes of a model; this implicit form of nonlinear NMI is particularly useful in models for which computing the horizontal normal modes is impracticable. The present paper extends the technique to the multilevel Canadian Operational Finite-Element Regional Model. This paper shows that the method yields well-balanced initial conditions and consistent vertical velocity fields. Forecasts from these initial conditions using a semi-Lagrangian time-integration scheme with relatively large time steps are free from unrealistic high-frequency oscillations.

1. Introduction

In a previous paper (Temperton 1988) an implicit form of nonlinear normal mode initialization (nonlinear NMI) was introduced. This procedure was designed for use in models whose normal modes cannot readily be found; for example, if the underlying linear equations are nonseparable. The success of the implicit nonlinear NMI technique was demonstrated in an application to a barotropic version of the Canadian Operational Finite-Element Regional Model. It has also been applied to a barotropic global spectral model (Temperton 1989), enabling a direct comparison to be made between the implicit scheme and the conventional nonlinear NMI procedure of Machenhauer (1977). For a mean depth of 5.6 km, it was shown that the two methods give essentially identical results, apart from small differences at the very largest horizontal scales.

This paper describes the application of an implicit nonlinear NMI scheme to the full multilevel version of the Canadian Finite-Element Regional Model (Staniforth and Daley 1979). Previously, the initialization for this model had been performed in a hemispheric spectral model with the same vertical discretization, after which the fields were horizontally interpolated to the grid of the regional model. This procedure, which required a rather delicate matching of the two models, was described by Verner and Benoit (1984). The idea of implicit nonlinear NMI was developed in order to provide a more direct (and more elegant) approach to initializing the regional model.

The "vertical mode" initialization (VMI) scheme of Bourke and McGregor (1983) is closely related to implicit NMI, but with a less complete treatment of the beta terms in the underlying linearization. Recently, McGregor and Bourke (1988) have compared the application of VMI in a limited-area model with a procedure analogous to that of Verner and Benoit (1984) in which initialized fields were interpolated from a hemispheric spectral model. They demonstrated that the two approaches gave similar results with some advantage for the more direct (VMI) procedure.

Temperton and Roch (1988) presented some results from a preliminary version of the multilevel implicit NMI procedure, which used vertical normal modes "borrowed" from another model (Béland and Beaudoin 1985) with a slightly different vertical discretization scheme. Since that time, the vertical discretization used in the operational regional model has itself undergone some changes in conjunction with the introduction of a semi-Lagrangian time-integration scheme (Tanguay et al. 1989). The opportunity was thus taken to make the vertical normal modes used in the initialization consistent with the new vertical discretization used in the model.

Section 2 of this paper describes the model, the discretization, and the vertical normal modes. The implicit nonlinear NMI scheme is described in section 3, and section 4 presents results. Section 5 includes the discussion and summary.

2. Discretization and vertical normal modes

The governing equations of the regional model are the hydrostatic primitive equations on a polar stereographic projection. The horizontal discretization is by bilinear finite elements using a variable mesh focused on the region of interest (Staniforth and Mitchell

---

1978). The vertical discretization is also by linear finite elements (Staniforth and Daley 1977), but as previously mentioned, there have been some recent changes in the details of the vertical formulation. The vertical coordinate is $\sigma = p/p_s$ (p is pressure, p_s is surface pressure). In the current operational configuration, there are 19 levels ranging from the model top at $\sigma_1 = 0.05$ to the surface at $\sigma_N = 1$ (note that $\sigma = \sigma_1$ and $\sigma = 1$ are both full model levels where all the prognostic variables are carried). The vertical boundary conditions are $\dot{\sigma} = 0$ at $\sigma = \sigma_1$ and at $\sigma = 1$.

The following will index the model levels by k, where $1 \leqslant k \leqslant N$ (here $N = 19$). For any variable v, $\mathbf{v}$ will denote the column vector

$$\mathbf{v} = (v_1, v_2, \cdots, v_N)^T$$

at a given horizontal position. The horizontal coordinates (on the stereographic projection) will be denoted by x and y.

As in Temperton (1988), the vorticity equation at each level may be written

$$\frac{\partial}{\partial t}(\nabla^2 \psi_k) = -\mathscr{I}\chi_k + (Q_\psi)_k \qquad (2.1)$$

where ψ is the streamfunction and χ is the velocity potential. The linear operators ∇^2, $\mathscr{I}$ are defined by

$$\nabla^2 \equiv \frac{\partial^2}{\partial x^2} + \frac{\partial^2}{\partial y^2},$$

$$\mathscr{I} \equiv \frac{\partial}{\partial x}\left(f\frac{\partial}{\partial x}\right) + \frac{\partial}{\partial y}\left(f\frac{\partial}{\partial y}\right)$$

where f is the Coriolis parameter. The nonlinear terms are grouped together in $(Q_\psi)_k$. In order to permit the introduction of an implicit NMI scheme, a small term $\mathscr{B}\psi_k$ on the right-hand side of (2.1), where the linear operator $\mathscr{B}$ is defined by

$$\mathscr{B} \equiv \frac{\partial}{\partial x}\left(f\frac{\partial}{\partial y}\right) - \frac{\partial}{\partial y}\left(f\frac{\partial}{\partial x}\right),$$

has been included with the nonlinear terms.

The divergence equation takes the form

$$\frac{\partial}{\partial t}(\nabla^2 \chi_k) = \mathscr{I}\psi_k + \mathscr{B}\chi_k - \nabla^2 P_k + (Q_\chi)_k \quad (2.2)$$

where P is an auxiliary variable given by

$$P_k = \varphi_k + RT^* \ln p_s, \qquad (2.3)$$

φ is the geopotential, R the gas constant, and T^* a reference temperature (assumed independent of model level).

The thermodynamic equation is

$$\frac{\partial T_k}{\partial t} - \left(\frac{\kappa T^*}{\sigma}\right)_k W_k = (Q_T)_k \qquad (2.4)$$

where $\kappa = R/c_p$ (c_p = specific heat of dry air), and W is an auxiliary variable related to the vertical velocity; thus in matrix/vector notation, (2.4) may be written

$$\frac{\partial \mathbf{T}}{\partial t} - \mathbf{KW} = \mathbf{Q}_T. \qquad (2.5)$$

The hydrostatic equation

$$\frac{\partial \varphi}{\partial \sigma} = -\frac{RT}{\sigma}$$

is vertically discretized as

$$\varphi_{k+1} - \varphi_k = (-1/2)R(T_{k+1} + T_k)\ln(\sigma_{k+1}/\sigma_k),$$
$$1 \leqslant k \leqslant N-1, \quad (2.6)$$

with $\varphi_N = \varphi_s$, the geopotential height of the orography. This aspect of the discretization departs from the standard Galerkin procedure used in the original version of the model by Staniforth and Daley (1979). Since φ_s is constant with time, (2.6) leads to an equation of the form

$$\frac{\partial \varphi}{\partial t} = \mathbf{G}\frac{\partial \mathbf{T}}{\partial t} \qquad (2.7)$$

where $\mathbf{G}$ is upper triangular with all entries zero on the last row. Combining (2.5) and (2.7) gives

$$\frac{\partial \varphi}{\partial t} - \mathbf{GKW} = \mathbf{Q}_\varphi. \qquad (2.8)$$

The auxiliary variable W is related to the horizontal divergence D by $D = -\partial W/\partial \sigma$. The associated vertical discretization is

$$(1/2)(D_k + D_{k+1}) = -(W_{k+1} - W_k)/(\sigma_{k+1} - \sigma_k),$$
$$1 \leqslant k \leqslant N-1, \quad (2.9)$$

with values of W at σ_1 and σ_N related by

$$W_1 = \sigma_1 W_N. \qquad (2.10)$$

In vector form,

$$\mathbf{W} = -\mathbf{MD} \qquad (2.11)$$

where the matrix $\mathbf{M}$ can be deduced from (2.9) and (2.10). Hence (2.8) becomes

$$\frac{\partial \varphi}{\partial t} + \mathbf{GKMD} = \mathbf{Q}_\varphi. \qquad (2.12)$$

The (vertically integrated) tendency equation for the surface pressure is

$$\frac{\partial}{\partial t}(\ln p_s) - W_N = Q_{(\ln p_s)}. \qquad (2.13)$$

Using (2.11), this can be written

$$\frac{\partial}{\partial t}(\ln p_s) + \eta^T \mathbf{D} = Q_{(\ln p_s)} \qquad (2.14)$$

where η^T is the last row of **M**. Now, in vector form (2.3) becomes

$$\mathbf{P} = \varphi + RT^*\mathbf{e} \ln p_s \qquad (2.15)$$

where **e** is a column vector $(1, 1, \ldots, 1)^T$. Combining (2.12), (2.14), and (2.15) results in an equation of the form

$$\frac{\partial \mathbf{P}}{\partial t} + \mathbf{C}\mathbf{D} = \mathbf{Q}_P \qquad (2.16)$$

where the matrix **C** is defined by

$$\mathbf{C} = \mathbf{G}\mathbf{K}\mathbf{M} + RT^*\mathbf{e}\eta^T. \qquad (2.17)$$

Finally, the divergence is related to the velocity potential through $D = m^2\nabla^2\chi$ where m is the map scale factor for the stereographic projection. Hence (2.16) becomes

$$\frac{\partial \mathbf{P}}{\partial t} = -m^2\mathbf{C}\nabla^2\chi + \mathbf{Q}_P. \qquad (2.18)$$

To determine the vertical normal modes, the vorticity and divergence equations (2.1) and (2.2) are rewritten in vector form:

$$\frac{\partial}{\partial t}(\nabla^2\psi) = -\mathcal{F}\chi + \mathbf{Q}_\psi \qquad (2.19)$$

$$\frac{\partial}{\partial t}(\nabla^2\chi) = \mathcal{F}\psi + \mathcal{B}\chi - \nabla^2\mathbf{P} + \mathbf{Q}_\chi. \qquad (2.20)$$

The vertical normal modes are then given by the decomposition

$$\mathbf{C} = \mathbf{E}\mathbf{\Phi}\mathbf{E}^{-1} \qquad (2.21)$$

where the columns of **E** are the eigenvectors of **C**, and **Φ** is a diagonal matrix,

$$\mathbf{\Phi} = \text{diag}(\Phi_1, \Phi_2, \cdots, \Phi_N).$$

Each column of **E** represents a vertical normal mode of the system (2.18)–(2.20), and is associated with an equivalent geopotential depth Φ_l.

Defining the vertical transforms

$$\hat{\mathbf{P}} = \mathbf{E}^{-1}\mathbf{P}, \quad \hat{\psi} = \mathbf{E}^{-1}\psi, \quad \hat{\chi} = \mathbf{E}^{-1}\chi \qquad (2.22)$$

and similarly for the nonlinear terms, premultiplying (2.18)–(2.20) by $\mathbf{E}^{-1}$ yields a set of equations for each vertical mode l:

$$\frac{\partial \hat{P}_l}{\partial t} = -m^2\Phi_l\nabla^2\hat{\chi}_l + (\hat{Q}_P)_l \qquad (2.23)$$

$$\frac{\partial}{\partial t}(\nabla^2\hat{\psi}_l) = -\mathcal{F}\hat{\chi}_l + (\hat{Q}_\psi)_l \qquad (2.24)$$

$$\frac{\partial}{\partial t}(\nabla^2\hat{\chi}_l) = \mathcal{F}\hat{\psi}_l + \mathcal{B}\hat{\chi}_l - \nabla^2\hat{P}_l + (\hat{Q}_\chi)_l. \qquad (2.25)$$

For each vertical mode, the set (2.23)–(2.25) has exactly the same form as the system of equations used to derive the implicit nonlinear NMI scheme for the

barotropic version of the regional finite-element model (Temperton 1988, section 5).

Notice here the choice to compute the vertical normal modes appropriate to the variables P, ψ, and χ (here ψ and χ could be replaced by vorticity and divergence, or by the components of the horizontal wind field). For a similar finite-element discretization in the vertical, Daley (1979) found a vertical structure equation in terms of the variable W and determined the normal modes of the discretized form of this equation. These vertical modes are different from those found here, but for a given underlying discretization the two sets of modes would be related through a similarity transformation.

For the purposes of the initialization scheme to be described in the following section, the vertical normal modes were determined using a reference temperature $T^* = 300$ K, the same as used in the model's semi-implicit time integration scheme. The equivalent depths $h_l = \Phi_l/g$ (g = acceleration due to gravity) are given in Table 1. Comparison with Table 1 of Verner and Benoit (1984) shows very close agreement for the first eight modes, in spite of the different number and positioning of levels and the changed vertical discretization. The vertical structure of the first six modes is shown in Fig. 1. These appear different from the corresponding modes presented by Daley (1979) or Verner and Benoit (1984), since as mentioned above they are appropriate for different variables; instead, they resemble the vertical modes presented by Temperton and Williamson (1981).
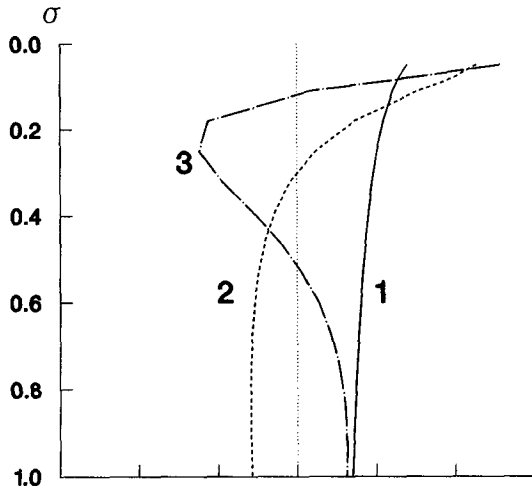
3. Initialization scheme

Using the vertical normal modes derived in the previous section, an implicit nonlinear NMI scheme for the multilevel regional finite-element model can be

TABLE 1. Equivalent depths.

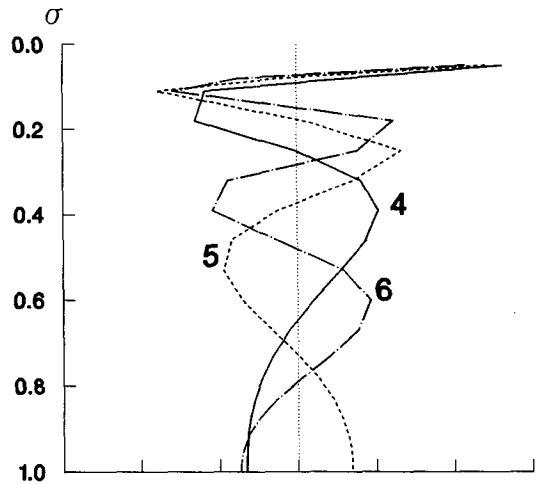| l	Equivalent depth h_l (m)
1	11172.04
2	1592.10
3	484.45
4	205.79
5	106.15
6	58.23
7	33.90
8	20.37
9	12.62
10	7.86
11	4.91
12	3.03
13	1.84
14	1.07
15	0.59
16	0.30
17	0.12
18	0.03
19	0.00

(a)

(b)

FIG. 1. The first six vertical modes of the model.

constructed. The generalization of the barotropic initialization algorithm of Temperton (1988) is analogous to that for conventional NMI in other models (e.g., Williamson and Temperton 1981) with a few technical differences resulting from the different vertical arrangement of the variables.

Each iteration of the scheme begins with a forward time step of the model to compute the tendencies:

$$\frac{\partial}{\partial t}(\nabla^2\psi), \quad \frac{\partial}{\partial t}(\nabla^2\chi), \quad \frac{\partial T}{\partial t}, \quad \frac{\partial}{\partial t}(\ln p_s).$$

The vertical transform (2.22) and the definition (2.15) of P are then used to compute

$$\frac{\partial}{\partial t}(\nabla^2\hat{\psi}_l), \quad \frac{\partial}{\partial t}(\nabla^2\hat{\chi}_l), \quad \frac{\partial \hat{P}_l}{\partial t} \qquad (3.1)$$

for as many vertical modes l as required. As in Temperton (1984), if the matrix $\mathbf{E}^{-1}\mathbf{G}$ and the column vector $RT^*\mathbf{E}^{-1}\mathbf{e}$ are precomputed, the explicit integration of the hydrostatic equation (2.6) can be avoided.

For each vertical mode to be initialized, the tendencies (3.1) are supplied to the initialization algorithm given in section 5 of Temperton (1988), with the vertical normal mode coefficients $\hat{\psi}_l$, $\hat{\chi}_l$, $\hat{P}_l$ replacing the original barotropic model variables ψ, χ, φ, respectively. For each vertical mode l there are several elliptic boundary value problems to be solved; the mean geopotential Φ, which appears in the elliptic operators in the barotropic case, is replaced by the appropriate equivalent geopotential depth Φ_l. Thus the changes $\Delta\hat{U}_l$, $\Delta\hat{V}_l$, and $\Delta\hat{P}_l$ are obtained for each vertical mode (U and V are the wind images).

The changes to the model wind fields are then determined via the vertical transforms

$$\Delta U = \mathbf{E}\Delta\hat{U}, \quad \Delta V = \mathbf{E}\Delta\hat{V}.$$

Obtaining the changes ΔT and $\Delta(\ln p_s)$ is slightly more subtle; the vertical transform

$$\Delta\mathbf{P} = \mathbf{E}\Delta\hat{\mathbf{P}} \qquad (3.2)$$

does not yield sufficient information. In models where the lowest level at which the prognostic variables are carried is *not* at the surface, there is a problem in separating ΔP into contributions $\Delta\varphi$ and $\Delta(\ln p_s)$. Temperton and Williamson (1981) discussed this problem as it appeared in the ECMWF model, and suggested a solution. In the case of the present model the problem manifests itself differently, but there is an analogous solution. First, since

$$P_N = \varphi_s + RT^* \ln p_s$$

and $\Delta\varphi_s = 0$, (3.2) implies

$$RT^*\Delta(\ln p_s) = \boldsymbol{\xi}^T\Delta\hat{\mathbf{P}} \qquad (3.3)$$

where $\boldsymbol{\xi}^T$ is the last row of $\mathbf{E}$. There is thus no ambiguity in defining $\Delta(\ln p_s)$. Using (2.15) and (3.2),

$$\Delta\varphi = \Delta\mathbf{P} - RT^*\mathbf{e}\Delta(\ln p_s)$$

can be obtained. The hydrostatic equation (2.6) implies

$$\mathbf{G}\Delta\mathbf{T} = \Delta\varphi; \qquad (3.4)$$

the problem is that $\mathbf{G}$ is singular (its last row is zero), so that (3.4) cannot be solved for $\Delta\mathbf{T}$.

We thus proceed as follows. The vertical normal modes are solutions of the equations in section 2 with the nonlinear terms set to zero. Thus, (2.5) together with (2.11) implies that the normal mode solutions satisfy

$$\frac{\partial\mathbf{T}}{\partial t} = -\mathbf{KMD}, \qquad (3.5)$$

while (2.16) together with (2.21) implies that they satisfy

$$\frac{\partial \mathbf{P}}{\partial t} = -\mathbf{E}\Phi\mathbf{E}^{-1}\mathbf{D}. \qquad (3.6)$$

Arguing as in Temperton and Williamson (1981), (3.5) and (3.6) together with (3.2) imply

$$\Delta \mathbf{T} = \mathbf{KME}\Phi^{-1}\Delta\hat{\mathbf{P}}. \qquad (3.7)$$

The problem remains that the diagonal matrix Φ is not invertible, since the last equivalent depth is zero. Thus, the last column of the matrix $\mathbf{KME}\Phi^{-1}$ is un-

defined. However, this does not matter since we are not initializing the last vertical mode, and hence the last component of $\Delta\hat{\mathbf{P}}$ is zero. To make the notation rigorous, (3.7) could be rewritten as

$$\Delta \mathbf{T} = \mathbf{KM} \sum_{l=1}^{m} (\Delta\hat{P}_l/\Phi_l)\mathbf{Z}_l \qquad (3.8)$$

where $\mathbf{Z}_l$ are the columns of $\mathbf{E}$, and the first m vertical modes are being initialized. It can be shown that if $\Delta(\ln p_s)$ is computed via (3.3) and $\Delta\mathbf{T}$ via (3.8), and the resulting
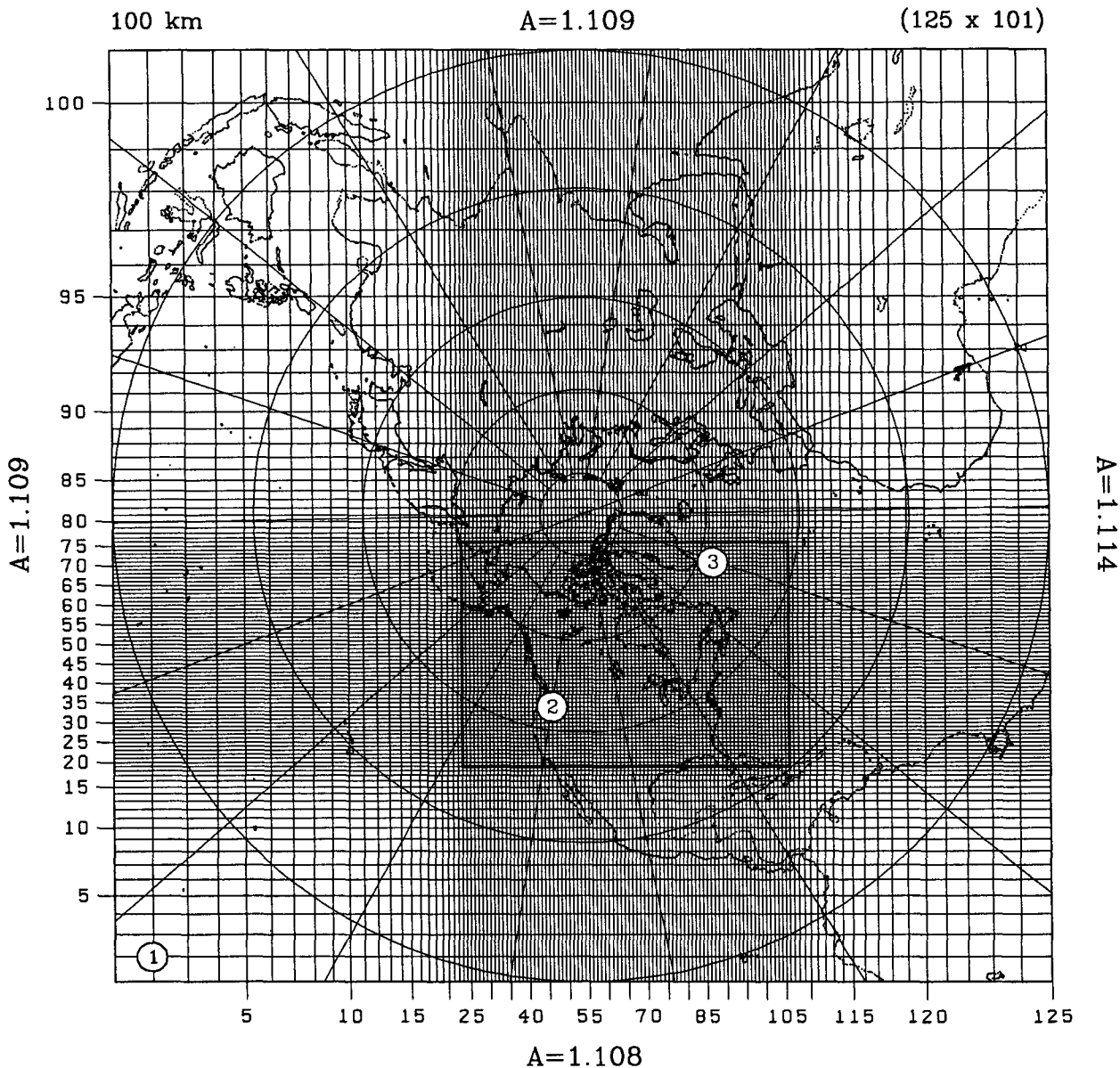

FIG. 2. The horizontal domain of the model showing the nonuniform grid. The numerals 1, 2, 3 indicate the position of grid points for which time traces of surface pressure are shown in Fig. 5.

$$\Delta \mathbf{P} = \mathbf{G}\Delta \mathbf{T} + RT^* e\Delta(\ln p_s)$$

is computed, then Eq. (3.2) is satisfied as required. The apparent ambiguity in defining ΔT has in effect been resolved by only allowing contributions from those vertical modes that are being initialized.

We have thus found the increments ΔU, ΔV, ΔT at each model level, and $\Delta(\ln p_s)$. The model variables can now be incremented, and the procedure may be iterated.

4. Results

The implicit normal mode initialization procedure described in section 3 has been implemented in the current operational version of the Canadian Finite-Element Regional Model. The semi-implicit semi-Lagrangian integration scheme used in this model was presented by Tanguay et al. (1989), while the parameterization of physical processes was described by Benoit et al. (1989). The horizontal domain and variable grid are shown in Fig. 2; over the central part of the grid, the horizontal resolution is 100 km. The lateral boundary is a solid wall tangent to the equator.

Initial conditions for the model are provided by interpolation from analyses defined on a hemispheric Gaussian grid, followed by a smoothing operation near the boundaries. The initialization scheme is run adiabatically, i.e., with all the physical processes turned off. In the first set of results to be presented here, the initial fields were taken from an archived FGGE analysis for 0000 UTC 21 December 1978.

First, the convergence of the initialization scheme is examined. As shown for example by Williamson and Temperton (1981), convergence problems may be encountered in conventional nonlinear NMI if too many vertical modes are initialized, and in practice normal mode initialization schemes are only applied for the first few vertical modes. In order to permit the development of an implicit NMI scheme, the underlying linear equations have to be slightly modified (the "beta" term in the vorticity equation is grouped with the nonlinear terms). Since this modification becomes more significant with decreasing equivalent depth, it is important to verify that the convergence of the initialization scheme for the first few internal vertical modes has not been adversely affected.

Williamson and Temperton (1981) examined the convergence of nonlinear NMI in terms of the parameter BAL, defined (for each vertical mode) as the sum of the squares of the tendencies of the fast mode coefficients. Since the initialization scheme is trying to reduce BAL to zero, its behavior as a function of the iteration number is a useful measure of convergence. As shown in Temperton (1988), BAL can also be computed during implicit NMI, though the individual fast mode tendencies are of course unknown.

The behavior of BAL for the multilevel finite-element regional model (starting from the FGGE analysis previously mentioned) is shown in Fig. 3 for two experiments, in which the number of vertical modes being initialized was respectively 3 and 6. The forward time steps, used to evaluate the tendencies of the model
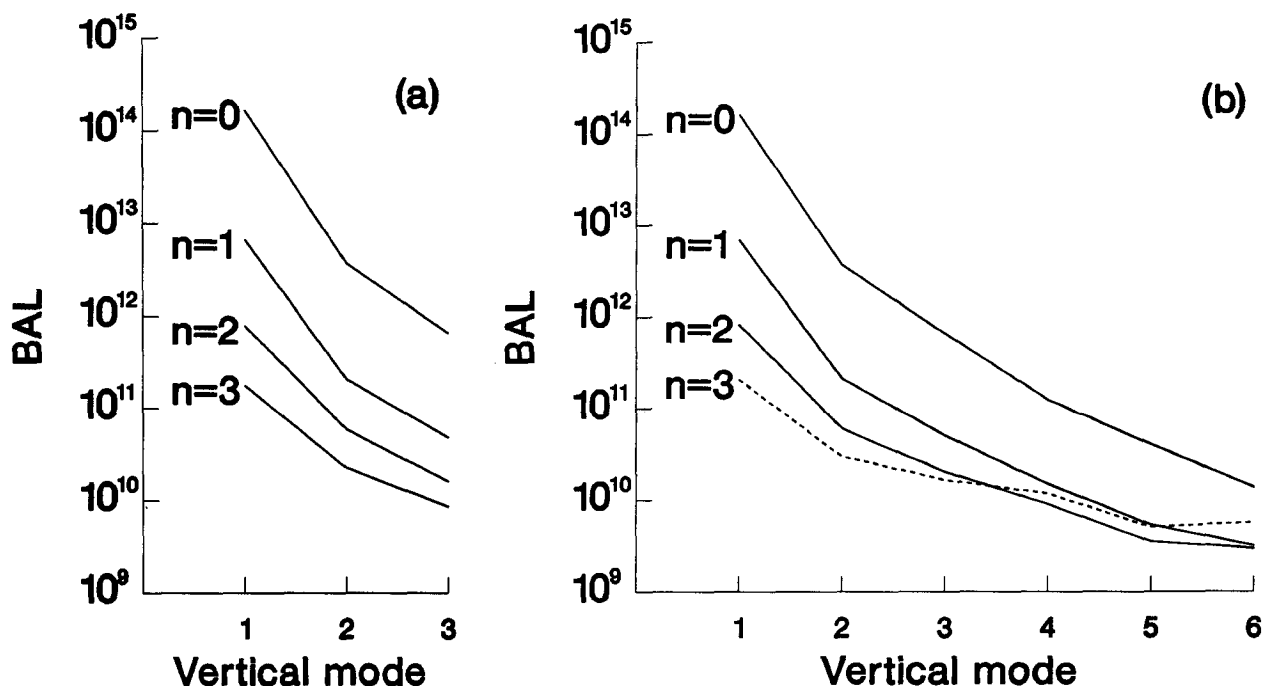

FIG. 3. The value of BAL for each vertical mode, after n iterations of implicit NMI. (a) Three vertical modes initialized; (b) six vertical modes initialized.
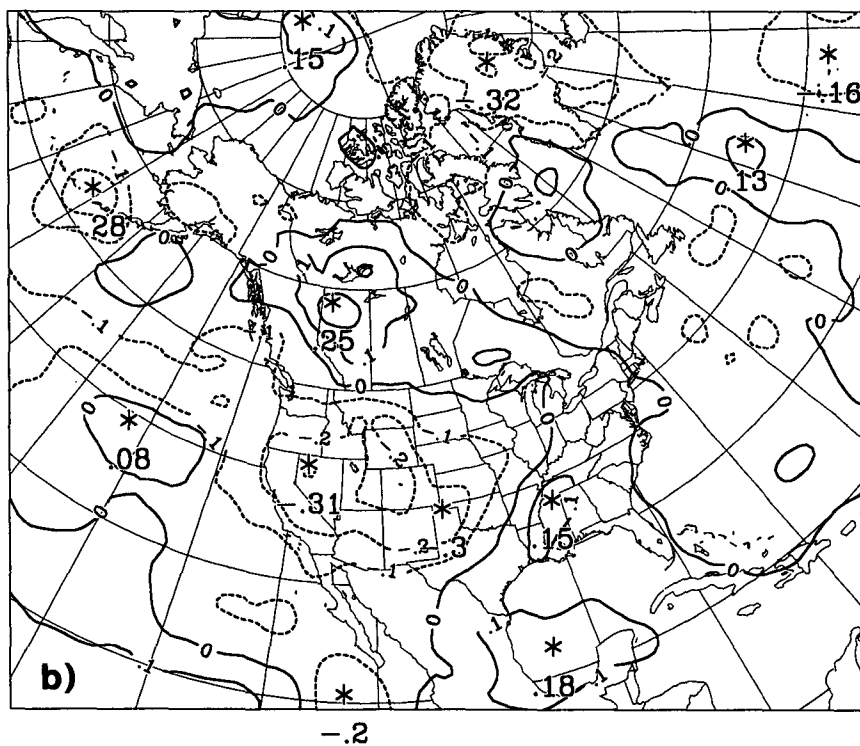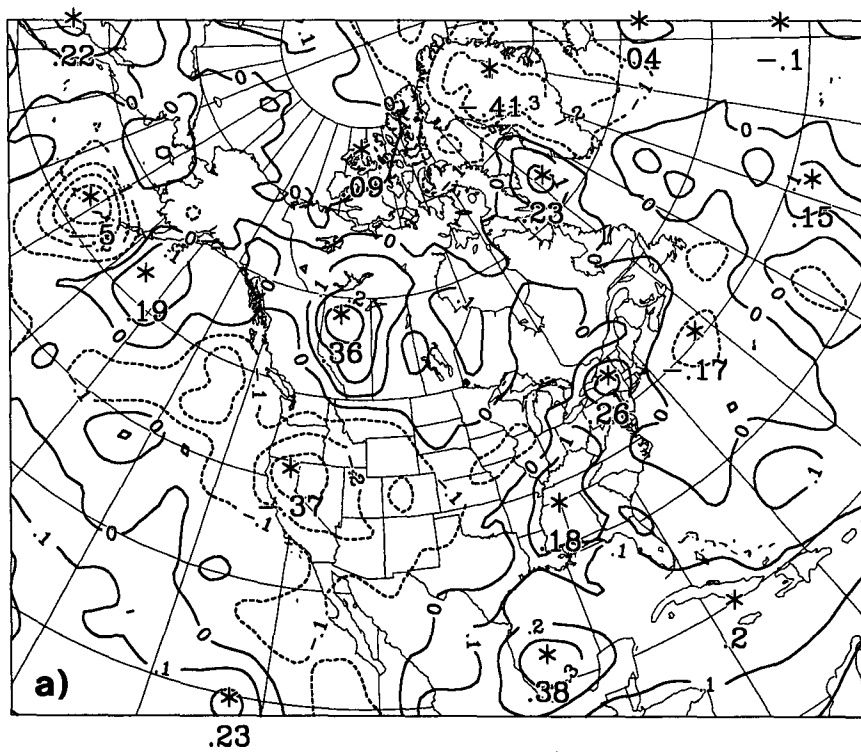
FIG. 4. Temperature changes due to initialization. (a) At $\sigma = 0.05$; (b) at $\sigma = 1$.
Contour interval is 0.1 deg.

variables for each iteration, were performed with the Eulerian (semi-implicit) version of the model dynamics and a time step of 120 s. It is clear that, in the case with three vertical modes being initialized, no convergence problems were encountered. When six vertical modes are initialized, the values for the shallower modes 4–6 begin to diverge on the third iteration. The behavior illustrated in Fig. 3 is similar to that seen during conventional nonlinear NMI. For operational implementation it was decided to run the initialization for three iterations and with three vertical modes; all subsequent results were obtained using this combination.

Another question requiring attention is the magnitude of the temperature changes (ΔT) produced by the initialization using (3.8). Although this is the only completely consistent way of obtaining ΔT, Daley (1979) reported that an analogous approach (in a model with a similar finite-element vertical discretization) yielded unacceptably large temperature changes; this led him to propose an alternative approach in which a variational integral was minimized. However, no such problems have been found with the scheme described here. Figure 4 shows the temperature changes over an area that includes the central (high-resolution) region of the model domain, both at the

model top ($\sigma = 0.05$) and at the surface ($\sigma = 1$). In both cases the changes are spatially coherent and certainly acceptably small (less than 0.5 deg everywhere).

These results confirm that the behavior of the implicit NMI scheme in this model is, as hoped, very similar to that of conventional NMI schemes in other multilevel models. It remains to be verified that the effect on the subsequent forecast is indeed to remove unwanted high-frequency oscillations. The fields obtained after three iterations, with three vertical modes initialized, were used as initial conditions for a 48-h forecast using the full model including a somewhat improved version of the physics package described by Benoit et al. (1989). This integration was compared with a similar forecast run directly from the uninitialized fields. Both forecasts used the semi-Lagrangian semi-implicit integration scheme of Tanguay et al. (1989), with a time step of 1200 s (the corresponding time step for an Eulerian version of the model at this resolution is 400 s).

Figure 5 shows the evolution of surface pressure at three selected points whose positions are indicated in Fig. 2. Point 1 is close to the corner of the domain, point 2 is close to the Rocky Mountains, while point 3 is over the ocean close to the edge of the high-resolution central area and not far from Greenland. At all
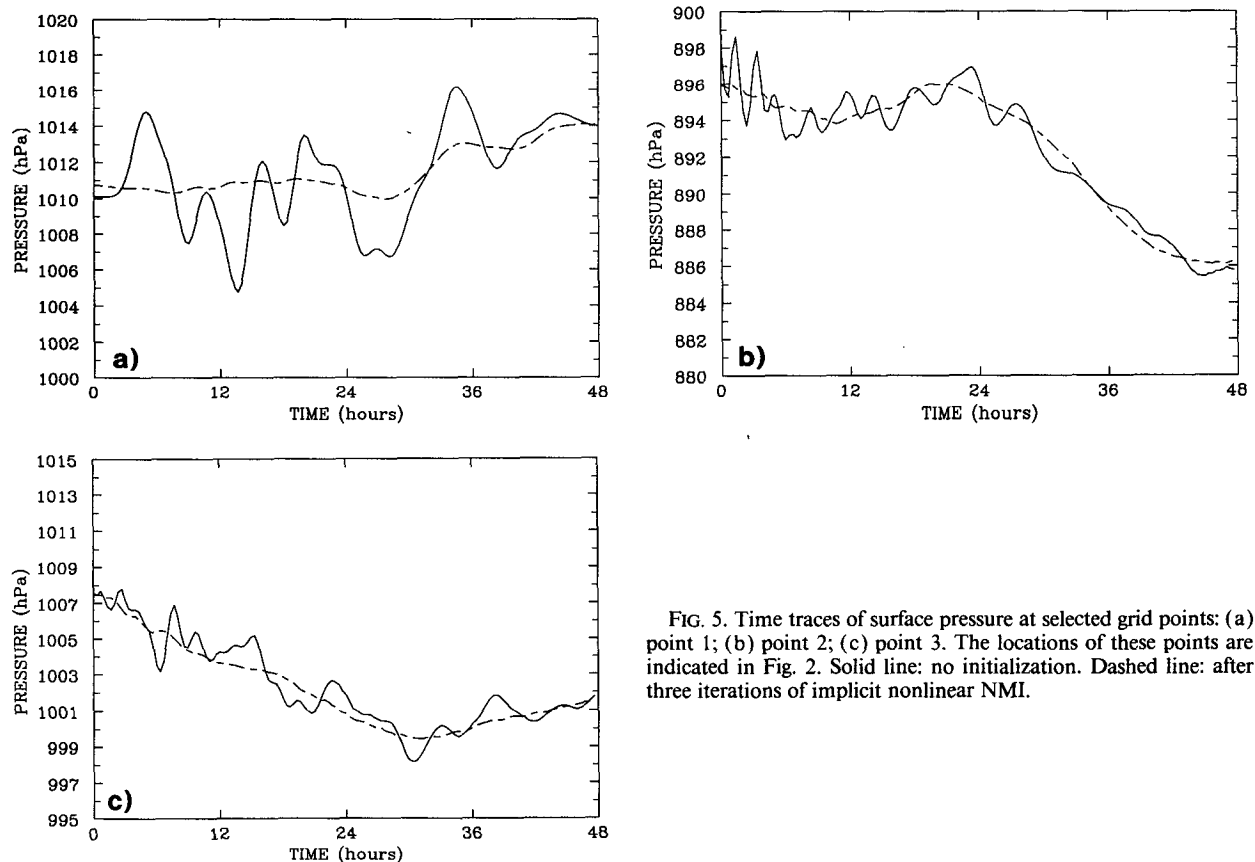

FIG. 5. Time traces of surface pressure at selected grid points: (a) point 1; (b) point 2; (c) point 3. The locations of these points are indicated in Fig. 2. Solid line: no initialization. Dashed line: after three iterations of implicit nonlinear NMI.
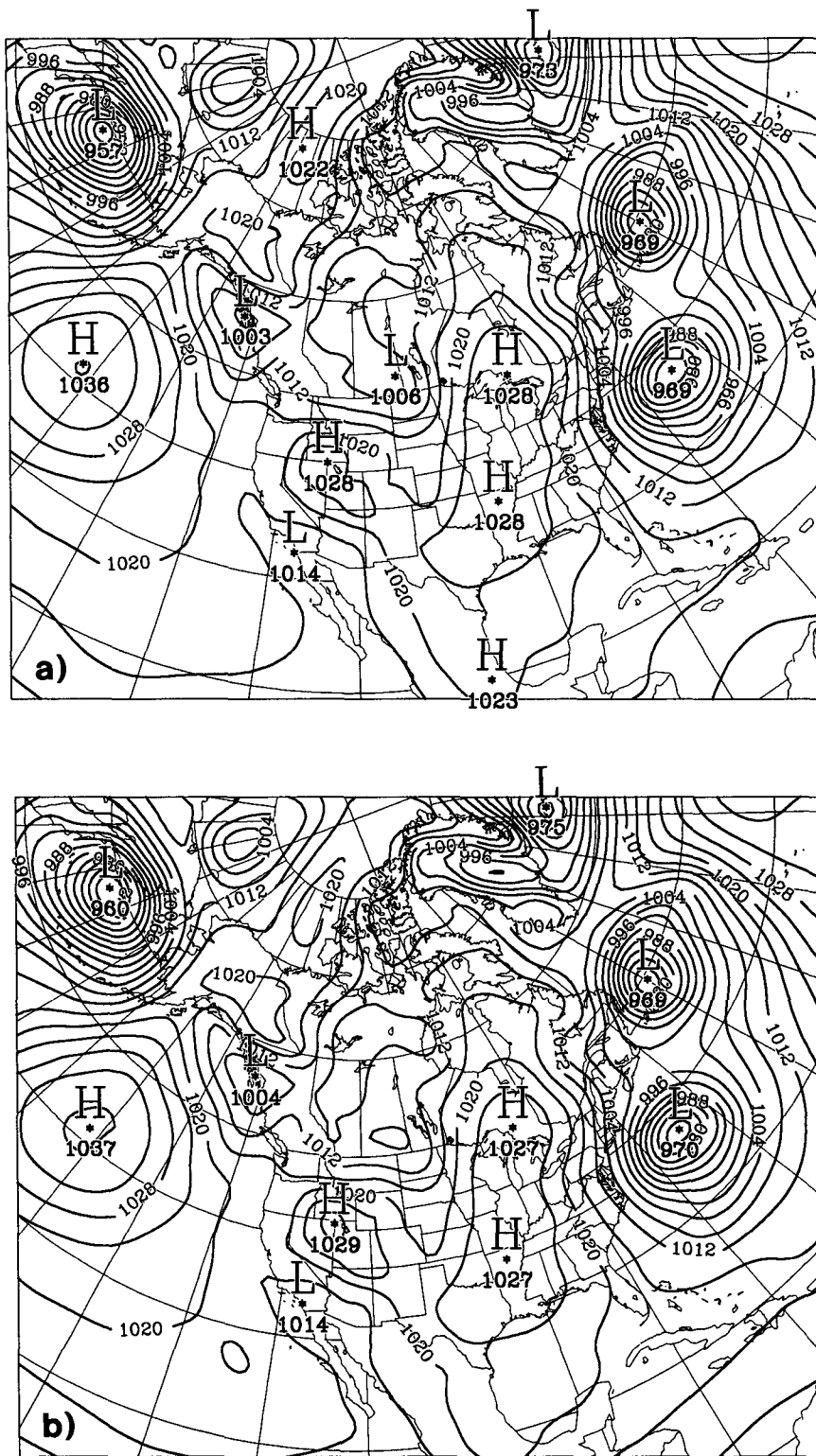
FIG. 6. Mean sea level pressure, 1200 UTC 4 January 1989, (a) before initialization; (b) after initialization. Contour interval is 4 hPa.
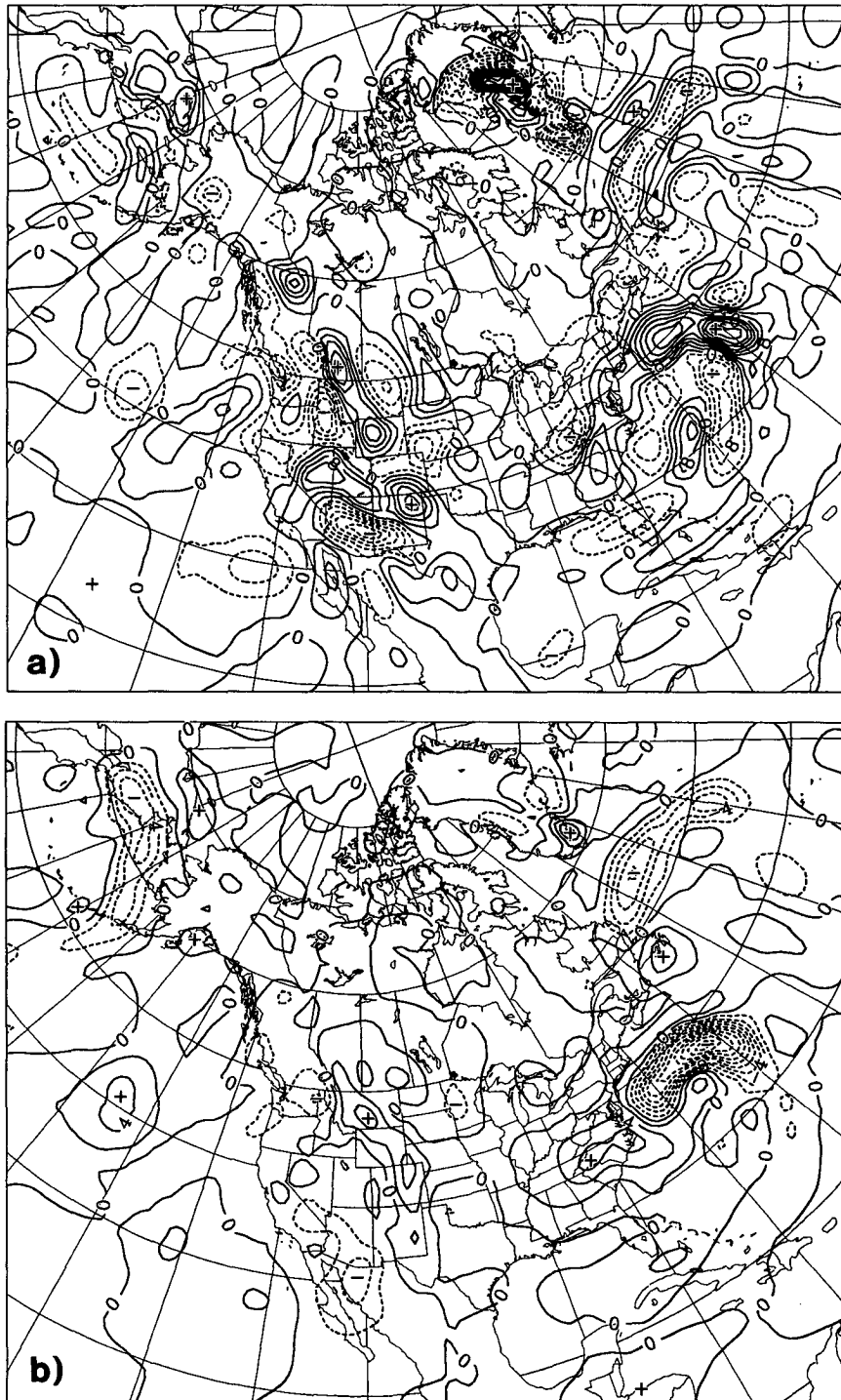
FIG. 7. Vertical velocity ω at 700 hPa, 1200 UTC 4 January 1989, (a) before initialization
(contour interval—4 μb s^{-1}); (b) after initialization (contour interval—2 μb s^{-1}).

three points the uninitialized forecast shows considerable high-frequency oscillations, with a peak-to-trough amplitude of as much as 10 hPa at point 1. In the initialized forecast the oscillations are almost completely absent, even at the selected points where difficulties might have been expected because of lateral boundaries or orographic forcing.

Thus, the impact of the implicit NMI scheme on the subsequent forecast is shown to be just as beneficial as that of conventional NMI. It is worth noting that

no special effort had to be made to take into account the fact that the forecast model uses a semi-Lagrangian scheme with relatively large time steps; an "Eulerian" initialization is quite sufficient.

In multilevel models an additional benefit of non-linear NMI is the generation of consistent fields of vertical motion in the initial conditions. To demonstrate the power of the implicit NMI scheme in this respect, an example from 1200 UTC on 4 January 1989 is given here. At this time, an explosively developing depression was situated in the western Atlantic. Figure 6 shows the sea level pressure over the area of interest, before and after initialization; the changes are generally of the order of 1 hPa, an acceptable degree of adjustment. Figure 7 shows the corresponding fields of vertical velocity ω at 700 hPa. Before initialization, this field is very disorganized and generally too intense. (The divergent component of the analyzed wind is kept in order to retain any useful information captured by the analysis scheme, particularly in the boundary layer.) After the initialization, and despite the neglect of diabatic effects, the vertical velocity field is much more coherent and synoptically reasonable; note in particular the pattern associated with the explosively deepening depression.

5. Summary and discussion

This paper has shown that the implicit nonlinear NMI scheme of Temperton (1988) can be extended to a multilevel model, thus enabling the benefits of NMI to be obtained in an operational regional model for which it is impracticable to compute the horizontal normal modes. The device of using another model to perform the initialization (Verner and Benoit 1984) becomes unnecessary, yielding a useful simplification of the operational forecast suite. The results presented here demonstrate that, in a multilevel model, the use of implicit nonlinear NMI provides balanced initial conditions including consistent vertical velocity fields, leading to a forecast uncontaminated by spurious high-frequency oscillations. It is of particular interest that these benefits are fully maintained when the forecast model uses a semi-Lagrangian time integration scheme.

A final step in validating the application of implicit nonlinear NMI in a multilevel model will be to perform a clean comparison between implicit and conventional NMI using a spectral model in which both approaches can be applied (Temperton 1989). A study along these lines is currently in progress and will form the subject of a future paper.

REFERENCES

Béland, M., and C. Beaudoin, 1985: A global spectral model with a finite-element formulation for the vertical discretization: Adiabatic formulation. *Mon. Wea. Rev.,* **113**, 1910–1919.

Benoit, R., J. Côté and J. Mailhot, 1989: Inclusion of a TKE boundary-layer parameterization in the Canadian regional finite-element model. *Mon. Wea. Rev.,* **117**, 1726–1750.

Bourke, W., and J. L. McGregor, 1983: A nonlinear vertical mode initialization scheme for a limited area prediction model. *Mon. Wea. Rev.,* **111**, 2285–2297.

Daley, R., 1979: The application of nonlinear normal mode initialization to an operational forecast model. Atmosphere: *Atmos. Ocean,* **17**, 97–124.

Machenhauer, B., 1977: On the dynamics of gravity oscillations in a shallow-water model, with application to normal mode initialization. *Contrib. Atmos. Phys.,* **50**, 253–271.

McGregor, J. L., and W. Bourke, 1988: A comparison of vertical mode and normal mode initialization. *Mon. Wea. Rev.,* **116**, 1320–1334.

Staniforth, A. N., and R. W. Daley, 1977: A finite-element formulation for the vertical discretization of sigma coordinate primitive equation models. *Mon. Wea. Rev.,* **105**, 1108–1118.

——, and H. L. Mitchell, 1978: A variable-resolution finite-element technique for regional forecasting with the primitive equations. *Mon. Wea. Rev.,* **106**, 439–447.

——, and R. W. Daley, 1979: A baroclinic finite-element model for regional forecasting with the primitive equations. *Mon. Wea. Rev.,* **107**, 107–121.

Tanguay, M., A. Simard and A. Staniforth, 1989: A three-dimensional semi-Lagrangian scheme for the Canadian regional finite-element forecast model. *Mon. Wea. Rev.,* **117**, 1861–1871.

Temperton, C., 1984: Orthogonal vertical normal modes for a multilevel model. *Mon. Wea. Rev.,* **112**, 503–509.

——, 1988: Implicit normal mode initialization. *Mon. Wea. Rev.,* **116**, 1013–1031.

——, 1989: Implicit normal mode initialization for spectral models. *Mon. Wea. Rev.,* **117**, 436–451.

——, and D. L. Williamson, 1981: Normal mode initialization for a multilevel grid point model. Part I: Linear aspects. *Mon. Wea. Rev.,* **109**, 729–743.

——, and M. Roch, 1988: Implicit normal mode initialization for an operational regional model. Preprints, *Eighth AMS Conference on Numerical Weather Prediction,* Baltimore, Amer. Meteor. Soc., 766–771.

Verner, G., and R. Benoit, 1984: Normal mode initialization of the RPN finite element model. *Mon. Wea. Rev.,* **112**, 1535–1543.

Williamson, D. L., and C. Temperton, 1981: Normal mode initialization for a multilevel grid point model. Part II: Nonlinear aspects. *Mon. Wea. Rev.,* **109**, 744–757.